Refined First-Order Shear Deformation Theory Models for Composite Laminates

F. Auricchio
Dipartimento di Meccanica Strutturale,
Università di Pavia,
Via Ferrata 1,
27100 Pavia, Italy
e-mail: auricchio@unipv.it

E. Sacco
Dipartimento di Meccanica, Stuutture, A. & T.,
Università di Cassino,
Via Di Biasio 43,
03043 Cassino, Italy
e-mail: sacco@unicas.it

In the present work, new mixed variational formulations for a first-order shear deformation laminate theory are proposed. The out-of-plane stresses are considered as primary variables of the problem. In particular, the shear stress profile is represented either by independent piecewise quadratic functions in the thickness or by satisfying the three-dimensional equilibrium equations written in terms of midplane strains and curvatures. The developed formulations are characterized by several advantages: They do not require the use of shear correction factors as well as the out-of-plane shear stresses can be derived without post-processing procedures. Some numerical applications are presented in order to verify the effectiveness of the proposed formulations. In particular, analytical solutions obtained using the developed models are compared with the exact three-dimensional solution, with other classical laminate analytical solutions and with finite element results. Finally, we note that the proposed formulations may represent a rational base for the development of effective finite elements for composite laminates.
[DOI: 10.1115/1.1572901]

1 Introduction

The modeling of composite laminated structures is one of the most active research fields of the last decades, since accurate stress analyses are required to design structural parts of mechanical, naval, aeronautical, and aerospace, as well as civil constructions.

In fact, composite laminates present an anisotropic response, with extension-bending coupling and non-negligible shear deformations in the thickness. Furthermore, to prevent the development of the delamination, which strongly limit the performances of composites, [1], an accurate evaluation of the interlaminar out-of-plane stresses (i.e., the shear stress and the normal stress in the thickness direction at the interface between two adjacent laminae) is required.

Actually, several laminate models are available in the literature, [2]. In particular, two different approaches may be distinguished in the laminate modeling, which lead to two classes of laminate theories: the equivalent single-layer theories (ESLTs) and the layerwise theories (LWTs).

The ESLTs represent the direct extension of plate theories to laminates, so that the laminate is reduced to a single-layer plate with equivalent anisotropic material properties. In fact, the classical laminate theory (CLT), [3,4], is an extension of the classical plate theory based on Kirchhoff-Love assumptions, i.e., it neglects the shear deformation in the thickness of the laminate. The first-order shear deformation theory (FSDT) is an extension of the Reissner, [5], and Mindlin, [6], plate models to the case of laminated anisotropic plates. The FSDT presented in Refs. [7,8] allows the determination of satisfactory solutions for a wide class of laminate problems. In particular, accurate results are obtained if proper values of the shear correction factors are adopted. Unfortunately, the exact values of the shear correction factors are known a priori only for very simple cases, [9]. To overcome this difficulty, two different approaches can be found in literature. The first approach consists in the development of iterative predictor-corrector techniques, as proposed by Noor and co-workers, [10–12]. Numerical procedures, developed within the finite element method, were proposed in Refs. [13,14], where new effective laminate elements were presented. The second approach is based on the refinement of the FSDT model, e.g., see Refs. [15,16]. Within this context, Rolfes and Rohwer [17] and Rolfes [18] proposed an improved composite finite element based on FSDT, which does not need the computation of the shear correction factors. They computed the transverse shear stresses from equilibrium equations and they were able to determine a priori the shear profile introducing suitable simplifications, i.e., neglecting the presence of membrane forces and assuming two simultaneous cylindrical bending modes.

Several higher-order shear deformation theories were developed in the literature, [19,20], within the ESLTs; they consider higher-order terms of the thickness coordinate in the representation form of the displacements.

The LWTs are obtained assuming independent shear deformation within each laminate layer, [21–25], so that the displacement field is continuous in the thickness, while the transverse shear strain can be discontinuous along the out-of-plane coordinate. The unknown functions for the LWTs depend on the number of layers in the laminate. A layerwise finite element formulation, which can be implemented in FEA commercial codes, was proposed in Ref. [26]; therein, Barbero discretized each layer in displacement-based three-dimensional elements with two-dimensional kinematic constraints.

The zig-zag theories are deduced from the LWT enforcing the continuity of the out-of-plane shear stresses; thus, the number of unknowns in the zig-zag theories do not depend on the number of layers, [27–30]. In particular, Carrera [30] developed multilayer and zig-zag theories in the framework of the Reissner mixed variational theorem.

Among the several laminate theories, the FSDT appears simple and efficient for many structural problems. In fact, as emphasized above, FSDT is able to predict the response of laminates with satisfactory approximations for most structural problems. On the other hand, finite element commercial codes, mainly based on displacement formulations, requires as input data the values of the shear correction factors. Moreover, the displacement formulations

Contributed by the Applied Mechanics Division of THE AMERICAN SOCIETY OF MECHANICAL ENGINEERS for publication in the ASME JOURNAL OF APPLIED MECHANICS. Manuscript received by the ASME Applied Mechanics Division, March 3, 2002; final revision, October 4, 2002. Associate Editor: M.-J. Pindera. Discussion on the paper should be addressed to the Editor, Prof. Robert M. McMeeking, Department of Mechanical and Environmental Engineering University of California–Santa Barbara, Santa Barbara, CA 93106-5070, and will be accepted until four months after final publication of the paper itself in the ASME JOURNAL OF APPLIED MECHANICS.

of plates and laminate theories are able to recover satisfactory values for the in-plane stresses, while out-of-plane shear and normal stresses are obtained after manipulations of the in-plane results by post-processing the solution, [13,14,31,32]. Post-processing techniques are generally simple and often efficient. Within finite element formulation the use of these techniques is not always straightforward. In fact, the determination of the shear stresses from equilibrium equations requires the computation of the in-plane stress (resultant axial forces and bending moments) derivatives. This can be accomplished developing mixed formulations, or displacement-based laminate finite elements characterized by high-degree polynomial interpolation functions, [13]. The stress derivatives can be also computed performing regularization of the extensional and flexural strain, [14]. The so-called extended two-dimensional method presented by Rolfes et al. [32] does not requires the computation of the stress derivatives; in fact, the assumption of neglecting the membrane forces and of considering the presence of two simultaneous cylindrical bending simplify the laminate equations, so that the bending moment derivatives are equal to the resultant shear stresses.

Furthermore, it can be emphasized that the FSDT allows to determine satisfactory values for the in-plane and out-of-plane stresses. Thus, once the most stressed zones of the laminate are determined using the FSDT, layerwise or zig-zig theories can be adopted in these zone to investigate on the possible delamination and failure.

Aim of the present paper is the development of suitable and viable laminate models based on the equivalent single layer theory. In particular, refined FSDT models, based on new partial mixed formulations, are developed, without introducing any simplification on the laminate problem.

The following features characterize the proposed approach:

- It does not need shear correction factors.
- It does not need to post-process the in-plane solution to get out-of-plane shear stresses.
- It may represent the basis for the development of new and efficient laminate finite elements.

The proposed approach is based on a variational formulation that considers the out-of-plane shear stresses as primarily variables of the problem. A new approach is proposed; in fact, the shear stress profile introduced in the partial mixed functional is obtained considering new independent variables or it is deduced from the three-dimensional local equilibrium equations. In fact, the explicit expression of the shear stresses is obtained by integrating the first two equilibrium equations with respect to the thickness direction. Thus, the shear stresses are expressed as functions of the in-plane stresses, which can be written as functions either of the in-plane strains or of the displacement and rotation fields. Hence, several formulations are obtained. In order to assess the performances of the proposed models, analytical solutions are determined for the proposed models. It can be emphasized that analytical solutions are available only for special cases; in fact, simply supported rectangular cross-ply and angle-ply laminates are considered within the paper. The solutions computed for the proposed models are compared with the exact three-dimensional solution, [33], with other classical laminate analytical solutions, [2], and with finite element results, [13].

In the following the subscript comma indicates the partial derivative $f_{,\alpha}=\partial f/\partial x_\alpha$ and $f_{,z}=\partial f/\partial z$.

2 First-Order Shear Deformation Theory (FSDT) Laminate Model

A laminate plate Ω refers to a flat body, with constant thickness h:

$$\Omega=\left\{(x_1,x_2,z)\in\mathcal{R}^3/z\in\left(-\frac{h}{2},\frac{h}{2}\right),(x_1,x_2)\in\mathcal{A}\subset\mathcal{R}^2\right\} \quad (1)$$

where the plane $z=0$ identifies the midplane $\mathcal{A}$ of the undeformed plate. The laminate is made of n layers and the typical kth layer lies between the thickness coordinates $z=z_k$ and $z=z_{k+1}$, such that $z_1=-h/2$ and $z_{n+1}=h/2$.

The first-order shear deformation theory can be obtained introducing suitable assumptions on both the strain and the stress fields defined in the three-dimensional continuous body Ω, as emphasized in [34] for the case of homogeneous plates. In fact, the FSDT for laminated plates is based on the following well-known assumptions, [35]:

1. The through-the-thickness transverse normal stress is nil, i.e., $\sigma_{zz}=0$.
2. Straight lines perpendicular to the midplane cannot be stretched, i.e., $\varepsilon_{zz}=0$.
3. Straight lines perpendicular to the midplane remain straight after deformation, i.e., $\varepsilon_{1z,z}=\varepsilon_{2z,z}=0$.

Displacement Field. The kinematics is restrained to satisfy the following conditions:

$$\varepsilon_{zz}=0 \quad \varepsilon_{1z,z}=\varepsilon_{2z,z}=0 \quad (2)$$

which leads to the classical representation form for the displacement field:

$$\mathbf{s}(x_1,x_2,z)=\mathbf{u}(x_1,x_2)+z\boldsymbol{\varphi}(x_1,x_2)$$
$$s_z(x_1,x_2,z)=w(x_1,x_2) \quad (3)$$

where

$$\mathbf{s}=\begin{Bmatrix}s_1\\s_2\end{Bmatrix} \quad \mathbf{u}=\begin{Bmatrix}u_1\\u_2\end{Bmatrix} \quad \boldsymbol{\varphi}=\begin{Bmatrix}\varphi_1\\\varphi_2\end{Bmatrix} \quad (4)$$

with $\mathbf{u}$ and $\boldsymbol{\varphi}$ the vectors of the midplane membrane displacements and rotations, respectively.

Strain Field. Denoting by ε_{ij} the typical component of the strain tensor, the in-plane strain vector $\boldsymbol{\varepsilon}=\{\varepsilon_{11}\ \varepsilon_{22}\ 2\varepsilon_{12}\}^T$, associated to the displacement representation (3), is written as

$$\boldsymbol{\varepsilon}=\mathbf{e}+z\boldsymbol{\kappa} \quad (5)$$

where the membrane strain vector $\mathbf{e}$ and the curvature strain vector $\boldsymbol{\kappa}$ are given by

$$\mathbf{e}=\mathbf{L}\mathbf{u} \quad \boldsymbol{\kappa}=\mathbf{L}\boldsymbol{\varphi} \quad \mathbf{L}=\begin{bmatrix}\dfrac{\partial}{\partial x_1} & 0\\ 0 & \dfrac{\partial}{\partial x_2}\\ \dfrac{\partial}{\partial x_2} & \dfrac{\partial}{\partial x_1}\end{bmatrix}. \quad (6)$$

The in-plane strain vector $\boldsymbol{\varepsilon}$ is a linear function of the thickness coordinate z.

The out-of-plane strain field vector $\boldsymbol{\gamma}=\{2\varepsilon_{1z}\ 2\varepsilon_{2z}\}^T$ is obtained as

$$\boldsymbol{\gamma}=\nabla w+\boldsymbol{\varphi} \quad (7)$$

where the symbol ∇ indicates the gradient operator.

Stress Field. The in-plane stresses within each lamina of the composite laminate are computed using the constitutive relationships. In particular, it is assumed that the body Ω is obtained assembling in a staking sequence orthotropic layers, with $z=0$ representing a plane of material symmetry. Thus, denoting by σ_{ij} the typical component of the stress tensor, the in-plane stress vector $\boldsymbol{\sigma}^k=\{\sigma_{11}^k\ \sigma_{22}^k\ \sigma_{12}^k\}^T$ for the kth lamina is given by

$$\boldsymbol{\sigma}^k=\mathbf{C}^k\boldsymbol{\varepsilon}=\mathbf{C}^k(\mathbf{e}+z\boldsymbol{\kappa}) \quad (8)$$

where $\mathbf{C}^k$ is the so-called reduced in-plane constitutive elastic matrix associated to the kth lamina. Note that $\mathbf{C}^k$ is derived from

the three-dimensional constitutive matrix, enforcing the condition 1, i.e., $\sigma_{zz}=0$, [34]. Since each lamina of the laminate presents different elastic properties, the in-plane stress vector $\boldsymbol{\sigma}$ is a discontinuous piecewise linear function of the coordinate z.

The out-of-plane shear stress vector $\boldsymbol{\theta}^k=\{\theta^k_{1z}\ \theta^k_{2z}\}^T$ can be evaluated through constitutive equation as

$$\boldsymbol{\theta}^k=\mathbf{Q}^k\gamma \tag{9}$$

where $Q^k_{\alpha\beta}=\chi_{\alpha\beta}\tilde{Q}^k_{\alpha\beta}$ with $\alpha,\beta=1,2$. Note that $\tilde{Q}^k_{\alpha\beta}$ are the components of the shear elastic matrix of the kth lamina and $\chi_{\alpha\beta}$ are the shear correction factors. As it is well known, the transverse shear stress vector computed by formula (9) is absolutely unsatisfactory; in fact, formula (9) leads to a transverse shear stress field which is not equilibrated at the interfaces of adjacent laminae and it does not satisfy the boundary conditions on the top and on the bottom of the laminate.

A satisfactory field for the out-of-plane shear stress vector $\boldsymbol{\tau}=\{\tau^k_{1z}\ \tau^k_{2z}\}^T$ can be recovered using the equilibrium equations; in the following no body forces and no tangential surface forces on the top and bottom of the laminate are considered; thus, the equilibrium equations give

$$\boldsymbol{\tau}=-\int_{-h/2}^{z}\mathbf{L}^T\boldsymbol{\sigma}d\varsigma, \tag{10}$$

i.e., in components

$$\tau_{\alpha z}=-\int_{-h/2}^{z}(\sigma_{\alpha 1,1}+\sigma_{\alpha 2,2})d\varsigma \quad \text{with} \quad \alpha=1,2. \tag{11}$$

Note that, according to formula (11), it implicitly results $\boldsymbol{\tau}(-h/2)=\mathbf{0}$; the further boundary condition $\boldsymbol{\tau}(h/2)=\mathbf{0}$ has also to be satisfied.

Once the shear stresses in the laminate thickness are determined, the transverse normal stress, which is very important for the delamination failure, can be determined adopting a post-processing method, i.e., by integrating with respect to z the third equilibrium equation:

$$\sigma_{zz}=-\int_{-h/2}^{z}(\tau_{1z,1}+\tau_{2z,2})d\varsigma. \tag{12}$$

It can be emphasized that the in-plane strain components (5) are linear functions of the z thickness coordinate, so that the in-plane stresses (8) are piecewise linear functions of z. As a consequence, the transverse shear stresses computed by the equilibrium Eq. (10) are piecewise quadratic functions. Since the piecewise quadratic shear stress profiles computed by Eq. (10) are widely recognized as the best transverse shear stresses evaluation, within the FSDT model, it can be assumed as basis for the model construction the condition that the through-the-thickness shear stresses $\sigma_{\alpha z}$ are continuous piecewise quadratic functions of the z-coordinate.

A classical problem arising in conjunction with the use of the FSDT is the determination of the shear factors χ_{11}, χ_{22}, and χ_{12} appearing in the matrix $\mathbf{Q}^k$ of Eq. (9). Denoting by $\mathcal{E}^\tau$ and $\mathcal{E}^\theta$ the complementary shear energies in the thickness obtained considering the $\boldsymbol{\tau}$ and $\boldsymbol{\theta}$ shear profiles, respectively, characterized by the same resultant shear stress, the shear correction factors are determined enforcing $\mathcal{E}^\tau=\mathcal{E}^\theta$. The exact values of χ_{11}, χ_{22}, and χ_{12} can be evaluated analytically only for special cases. In particular, Whitney [9] derived an analytical formula of the shear correction factor for the case of cross-ply laminates in cylindrical bending. For a more general case, it is possible to evaluate the shear correction factors developing an iterative procedure. This can be based on the determination of the displacement solution, of in-plane stresses computation via constitutive equations, of the equilibrated shear stresses, of the complementary shear energies and, finally, of new shear correction factors which are adopted to compute a new solution, and so on, [13].

3 Variational Formulation

A mixed functional for the three-dimensional laminate-like body Ω is now considered:

$$H(\mathbf{u},w,\boldsymbol{\varphi},\mathbf{e},\boldsymbol{\kappa},\boldsymbol{\gamma},\boldsymbol{\sigma},\boldsymbol{\tau})=H^{mb}(\mathbf{u},\boldsymbol{\varphi},\mathbf{e},\boldsymbol{\kappa},\boldsymbol{\sigma})+H^s(w,\boldsymbol{\varphi},\boldsymbol{\gamma},\boldsymbol{\tau})-\Pi_{\text{ext}} \tag{13}$$

where H^{mb} is a Hu-Washizu functional accounting for the membrane-bending terms, H^s is a Prange-Hellinger-Reissner functional accounting for the transverse shear terms and Π_{ext} accounts for the boundary conditions and loading forces.

In particular, the membrane-bending functional H^{mb} and the transverse shear functional H^s are written as

$$H^{mb}(\mathbf{u},\boldsymbol{\varphi},\mathbf{e},\boldsymbol{\kappa},\boldsymbol{\sigma})=\frac{1}{2}\int_\Omega(\mathbf{e}+z\mathbf{k})^T\mathbf{C}(\mathbf{e}+z\boldsymbol{\kappa})dv + \int_\Omega[(\mathbf{L}\mathbf{u}-\mathbf{e})+z(\mathbf{L}\boldsymbol{\varphi}-\boldsymbol{\kappa})]^T\boldsymbol{\sigma}dv \tag{14}$$

$$H^s(w,\boldsymbol{\varphi},\boldsymbol{\tau})=\int_\Omega(\nabla w+\boldsymbol{\varphi})^T\boldsymbol{\tau}dv-\frac{1}{2}\int_\Omega\boldsymbol{\tau}^T\mathbf{T}\boldsymbol{\tau}dv \tag{15}$$

where $\mathbf{T}^k=(\mathbf{Q}^k)^{-1}$ is the shear compliance matrix of the kth layer.

Performing the integration along the thickness coordinate, the membrane-bending mixed functional (14) takes the form

$$\tilde{H}^{mb}(\mathbf{u},\boldsymbol{\varphi},\mathbf{e},\boldsymbol{\kappa},\mathbf{N},\mathbf{M})=\frac{1}{2}\int_{\mathcal{A}}(\mathbf{e}^T\mathbf{A}\mathbf{e}+2\mathbf{e}^T\mathbf{B}\boldsymbol{\kappa}+\boldsymbol{\kappa}^T\mathbf{D}\boldsymbol{\kappa})dA + \int_{\mathcal{A}}\{[(\mathbf{L}\mathbf{u})-\mathbf{e}]^T\mathbf{N}+[(\mathbf{L}\boldsymbol{\varphi})-\boldsymbol{\kappa}]^T\mathbf{M}\}dA. \tag{16}$$

The matrices $\mathbf{A}$, B, and $\mathbf{D}$ represent the membrane, the membrane-bending coupling and the bending elastic stiffness matrices of a n layer laminate, respectively, defined by equations

$$\mathbf{A}=\sum_{k=1}^{n}\mathbf{C}^k(z_{k+1}-z_k) \tag{17}$$

$$\mathbf{B}=\frac{1}{2}\sum_{k=1}^{n}\mathbf{C}^k(z^2_{k+1}-z^2_k) \tag{18}$$

$$\mathbf{D}=\frac{1}{3}\sum_{k=1}^{n}\mathbf{C}^k(z^3_{k+1}-z^3_k). \tag{19}$$

Moreover, the resultant membrane force and bending moment vectors, $\mathbf{N}$ and $\mathbf{M}$, are defined as

$$\mathbf{N}=\int_{-h/2}^{h/2}\boldsymbol{\sigma}dz \quad \mathbf{M}=\int_{-h/2}^{h/2}z\boldsymbol{\sigma}dz. \tag{20}$$

Because of the constitutive Eqs. (8), taking into account the definitions (17), (18), and (19), it results:

$$\mathbf{N}=\mathbf{A}\mathbf{e}+\mathbf{B}\boldsymbol{\kappa} \quad \mathbf{M}=\mathbf{B}\mathbf{e}+\mathbf{D}\boldsymbol{\kappa}. \tag{21}$$

Hence, the mixed functional (13) for the laminate can be written in terms of the introduced resultant forces and bending moments as

$$\tilde{H}(\mathbf{u},w,\boldsymbol{\varphi},\mathbf{e},\boldsymbol{\kappa},\boldsymbol{\gamma},\mathbf{N},\mathbf{M},\boldsymbol{\tau})=\tilde{H}^{mb}(\mathbf{u},\boldsymbol{\varphi},\mathbf{e},\boldsymbol{\kappa},\mathbf{N},\mathbf{M}) + H^s(w,\boldsymbol{\varphi},\boldsymbol{\gamma},\boldsymbol{\tau})-\Pi_{\text{ext}}. \tag{22}$$

A full displacement formulation of the membrane-bending functional $\tilde{H}^{mb}$ is recovered, implicitly satisfying the resultant constitutive laws (21) and the compatibility Eqs. (6):

$$\mathcal{E}^{mb}(\mathbf{u},\boldsymbol{\varphi})=\frac{1}{2}\int_{\mathcal{A}}[(\mathbf{Lu})^T\mathbf{ALu}+2(\mathbf{Lu})^T\mathbf{BL}\boldsymbol{\varphi}+(\mathbf{L}\boldsymbol{\varphi})^T\mathbf{DL}\boldsymbol{\varphi}]dA. \tag{23}$$

It can be emphasized that different laminate models can be recovered depending on the expression considered for the through-the-thickness shear stress. In particular, two classes of models are herein considered:

- The shear stress profile are approximated introducing independent variables.
- The shear stress profile are written as function of the midplane strains and curvatures using the equilibrium Eqs. (10).

In the following, four variational formulations of the laminate problem are derived, considering different representation forms of the out-of-plane shear stress vector.

4 Independent Approximation of the Shear Stresses

The first refined model, denoted in the following as RM1, is derived considering independent approximations of the shear stresses. In fact, the shear stress profile is represented as a continuous piecewise quadratic function in the thickness, satisfying the boundary conditions. Hence, within the kth layer, it is assumed

$$\boldsymbol{\tau}^k=\mathbf{t}_o^k\frac{z_{k+1}-z}{z_{k+1}-z_k}+\mathbf{t}_o^{k+1}\frac{z-z_k}{z_{k+1}-z_k}-\mathbf{t}^k(z_{k+1}-z)(z-z_k) \tag{24}$$

with $\mathbf{t}_o^1=\mathbf{t}_o^{n+1}=\mathbf{0}$. In the formula (24) $\mathbf{t}_o^k$ represents the shear stress vector at the interface between the layers $k-1$ and k, while $\mathbf{t}^k$ gives the curvature profile of the shear stress in kth layer.

Introducing the representation formula (24) in the transverse shear energy (15), it applies

$$\begin{aligned}\tilde{H}^s=&-\frac{1}{2}\int_{\mathcal{A}}\sum_{k=1}^{n}\left[(\mathbf{R}^k\mathbf{t}_o^k)^T\mathbf{t}_o^k+(\mathbf{R}^k\mathbf{t}_o^{k+1})^T\mathbf{t}_o^k-(\tilde{\mathbf{R}}^k\mathbf{t}^k)^T\mathbf{t}_o^k\right]dA\\&+-\frac{1}{2}\int_{\mathcal{A}}\sum_{k=1}^{n}\left[(\mathbf{R}^k\mathbf{t}_o^{k+1})^T\mathbf{t}_o^{k+1}-(\tilde{\mathbf{R}}^k\mathbf{t}^k)^T\mathbf{t}_o^{k+1}\right]dA\\&+-\frac{1}{2}\int_{\mathcal{A}}\sum_{k=1}^{n}[(\hat{\mathbf{R}}^k\mathbf{t}^k)^T\mathbf{t}^k]dA+\int_{\mathcal{A}}(\nabla w\\&+\boldsymbol{\varphi})^T\sum_{k=1}^{n}\frac{z_{k+1}-z_k}{2}\left(\mathbf{t}_o^k+\mathbf{t}_o^{k+1}-\mathbf{t}^k\frac{(z_{k+1}-z_k)^2}{3}\right)dA\end{aligned} \tag{25}$$

where

$$\mathbf{R}^k=\frac{z_{k+1}-z_k}{3}\mathbf{T}^k\quad\tilde{\mathbf{R}}^k=\frac{(z_{k+1}-z_k)^3}{6}\mathbf{T}^k\quad\hat{\mathbf{R}}^k=\frac{(z_{k+1}-z_k)^5}{30}\mathbf{T}^k. \tag{26}$$

Finally, the mixed functional (22) takes the form

$$\begin{aligned}&\hat{H}(\mathbf{u},w,\boldsymbol{\varphi},\mathbf{e},\boldsymbol{\kappa},\mathbf{N},\mathbf{M},\mathbf{t}_o^2,..,\mathbf{t}_o^n,\mathbf{t}^1,..,\mathbf{t}^n)\\&\quad=\tilde{H}^{mb}(\mathbf{u},\boldsymbol{\varphi},\mathbf{e},\boldsymbol{\kappa},\mathbf{N},\mathbf{M})+\hat{H}^s(w,\boldsymbol{\varphi},\mathbf{t}_o^2,..,\mathbf{t}_o^n,\mathbf{t}^1,..,\mathbf{t}^n)-\Pi_{\text{ext}}.\end{aligned} \tag{27}$$

The number of the unknowns in the FSDT refined model RM1 depends on the number of layers. Since the transverse shear stress profile does not depend on the in-plane stresses, the membrane and bending terms can be written adopting a full displacement approach functional, substituting $\tilde{H}^{mb}$ with $\mathcal{E}^{mb}$ in Eq. (27).

The presented approach leads to serious drawbacks. In fact, the stationary condition of the mixed functional (22) with respect to the shear stress τ gives

$$0=\partial_\tau H^s(w,\boldsymbol{\varphi},\boldsymbol{\tau})=\int_\Omega(\nabla w+\boldsymbol{\varphi})^T\delta\boldsymbol{\tau}dv-\frac{1}{2}\int_\Omega\boldsymbol{\tau}^T\mathbf{T}\delta\boldsymbol{\tau}dv \tag{28}$$

i.e., $\mathbf{T}^k\boldsymbol{\tau}^k=\nabla w+\boldsymbol{\varphi}$; thus, Eq. (28) represents the complementary constitutive equation written in variational form. Because of the displacement representation form (3) for the FSDT, the second term of Eq. (28) is constant in the thickness, so that the shear stress vector τ is enforced to be piecewise constant in the thickness. When the stress τ is represented by formula (24), the variational Eq. (28) enforces the constitutive law in approximated form; enlarging the space of the shear parameters $\mathbf{t}_o^2,..,\mathbf{t}_o^n,\mathbf{t}^1,..,\mathbf{t}^n$, i.e., increasing the number of independent parameters defining the stress $\boldsymbol{\tau}$ given by formula (24), the constitutive Eq. (28) tends to be enforced in a stronger manner, so that the shear stress profile tends to become piecewise constant in the laminate thickness.

5 Equilibrated Shear Stress

5.1 Shear Stress Computation. The out-of-plane shear stress $\boldsymbol{\tau}$, computed using the equilibrium Eqs. (10), is a continuous piecewise quadratic function of the thickness coordinate; thus, the transverse shear stress $\boldsymbol{\tau}^k$ at the kth lamina is given by

$$\boldsymbol{\tau}^k(z)=-\int_{z_k}^{z}\mathbf{L}^T\boldsymbol{\sigma}^k d\varsigma+\boldsymbol{\tau}_o^k \tag{29}$$

where $\boldsymbol{\tau}_o^k$ is the stress evaluated at $z=z_k$:

$$\boldsymbol{\tau}_o^k=-\int_{-h/2}^{z_k}\mathbf{L}^T\boldsymbol{\sigma}d\varsigma. \tag{30}$$

Substituting the expression (8) into the formula (30) gives

$$\boldsymbol{\tau}_o^k=-\int_{-h/2}^{z_k}\mathbf{L}^T\mathbf{C}(\mathbf{e}+\varsigma\boldsymbol{\kappa})d\varsigma=-\mathbf{L}^T(\hat{\mathbf{A}}^k\mathbf{e}+\hat{\mathbf{B}}^k\boldsymbol{\kappa}) \tag{31}$$

with

$$\hat{\mathbf{A}}^k=\sum_{i=1}^{k-1}\mathbf{C}^i(z_{i+1}-z_i)\quad\hat{\mathbf{B}}^k=\frac{1}{2}\sum_{i=1}^{k-1}\mathbf{C}^i(z_{i+1}^2-z_i^2). \tag{32}$$

Then, taking into account expressions (8) and (31) and performing the integration in the thickness, the out-of-plane shear stress $\boldsymbol{\tau}^k$ (29) becomes

$$\begin{aligned}\boldsymbol{\tau}^k(z)&=-\mathbf{L}^T\left[(z-z_k)\mathbf{C}^k\mathbf{e}+\frac{1}{2}(z^2-z_k^2)\mathbf{C}^k\boldsymbol{\kappa}\right]-\mathbf{L}^T(\hat{\mathbf{A}}^k\mathbf{e}+\hat{\mathbf{B}}^k\boldsymbol{\kappa})\\&=-\mathbf{L}^T(\mathbf{A}^k(z)\mathbf{e}+\mathbf{B}^k(z)\boldsymbol{\kappa})\end{aligned} \tag{33}$$

where

$$\begin{aligned}\mathbf{A}^k(z)&=(z-z_k)\mathbf{C}^k+\hat{\mathbf{A}}^k\\\mathbf{B}^k(z)&=\frac{1}{2}(z^2-z_k^2)\mathbf{C}^k+\hat{\mathbf{B}}^k.\end{aligned} \tag{34}$$

Moreover, in order to satisfy the boundary condition $\boldsymbol{\tau}(h/2)=\mathbf{0}$ exactly, the formula (33) is enhanced by adding a linear term which is zero at $z=-h/2$:

$$\boldsymbol{\tau}^k(z)=-\mathbf{L}^T(\mathbf{A}^k(z)\mathbf{e}+\mathbf{B}^k(z)\boldsymbol{\kappa})+\mathbf{a}\left(z+\frac{1}{2}h\right). \tag{35}$$

The vector $\mathbf{a}$ is evaluated enforcing the boundary condition:

$$\mathbf{0}=\boldsymbol{\tau}^n(h/2)=-\mathbf{L}^T(\mathbf{Ae}+\mathbf{B}\boldsymbol{\kappa})+\mathbf{a}h \tag{36}$$

where $\mathbf{A}^n(h/2)=\mathbf{A}$ and $\mathbf{B}^n(h/2)=\mathbf{B}$ are the membrane and membrane-bending coupling elastic matrices of the laminate defined by Eqs. (17) and (18), respectively. Solving Eq. (36) with respect to the vector $\mathbf{a}$, we obtain

$$\mathbf{a}=\frac{1}{h}\mathbf{L}^T(\mathbf{A}\mathbf{e}+\mathbf{B}\boldsymbol{\kappa}). \tag{37}$$

Substituting expression (37) into formula (35), the out-of-plane shear stress $\boldsymbol{\tau}^k$ takes the form

$$\boldsymbol{\tau}^k(z)=-\mathbf{L}^T\left\{\left[\mathbf{A}^k(z)-\frac{1}{h}\left(z+\frac{1}{2}h\right)\mathbf{A}\right]\mathbf{e}+\left[\mathbf{B}^k(z)-\frac{1}{h}\left(z+\frac{1}{2}h\right)\mathbf{B}\right]\boldsymbol{\kappa}\right\}. \tag{38}$$

A suitable form for the expression of the out-of-plane shear stress $\boldsymbol{\tau}^k$, useful for the next developments, is proposed. In fact, the formula (38) can be rewritten in the following equivalent form:

$$\boldsymbol{\tau}^k(z)=-\mathbf{L}^T[(\mathbf{A}^{k(0)}+z\mathbf{A}^{k(1)})\mathbf{e}+(\mathbf{B}^{k(0)}+z\mathbf{B}^{k(1)}+z^2\mathbf{B}^{k(2)})\boldsymbol{\kappa}] \tag{39}$$

where

$$\mathbf{A}^{k(0)}=\hat{\mathbf{A}}^k-z_k\mathbf{C}^k-\frac{1}{2}\mathbf{A}\quad \mathbf{A}^{k(1)}=\mathbf{C}^k-\frac{1}{h}\mathbf{A} \tag{40}$$

$$\mathbf{B}^{k(0)}=\hat{\mathbf{B}}^k-\frac{1}{2}z_k^2\mathbf{C}^k-\frac{1}{2}\mathbf{B}\quad \mathbf{B}^{k(1)}=-\frac{1}{h}\mathbf{B}\quad \mathbf{B}^{k(2)}=\frac{1}{2}\mathbf{C}^k. \tag{41}$$

Next, several refined FSDT laminate formulations, based on the use of equilibrated shear stresses, are derived.

5.2 Refined Model RM2. The FSDT refined model RM2 is deduced substituting the expression (39) of the transverse shear stress vector $\boldsymbol{\tau}$, obtained from the three-dimensional equilibrium equations, into the mixed shear functional $\tilde{H}^s$ defined in (15). Thus,

$$\begin{aligned}\overline{\tilde{H}}^s=&\int_{\mathcal{A}}\sum_{k=1}^{n}\left\{\frac{1}{2}\mathbf{T}^k\mathbf{L}^T\mathbf{X}^{k(0)}\mathbf{e}+\mathbf{T}^k\mathbf{L}^T\mathbf{Y}^{k(0)}\boldsymbol{\kappa}\right\}^T\mathbf{L}^T\mathbf{A}^{k(0)}\mathbf{e}dA+\int_{\mathcal{A}}\sum_{k=1}^{n}\left\{\frac{1}{2}\mathbf{T}^k\mathbf{L}^T\mathbf{X}^{k(1)}\mathbf{e}+\mathbf{T}^k\mathbf{L}^T\mathbf{Y}^{k(1)}\boldsymbol{\kappa}\right\}^T\mathbf{L}^T\mathbf{A}^{k(1)}\mathbf{e}dA\\&+\frac{1}{2}\int_{\mathcal{A}}\sum_{k=1}^{n}[\mathbf{T}^k\mathbf{L}^T\mathbf{Y}^{k(0)}\boldsymbol{\kappa}]^T\mathbf{L}^T\mathbf{B}^{k(0)}\boldsymbol{\kappa}dA+\frac{1}{2}\int_{\mathcal{A}}\sum_{k=1}^{n}[\mathbf{T}^k\mathbf{L}^T\mathbf{Y}^{k(1)}\boldsymbol{\kappa}]^T\mathbf{L}^T\mathbf{B}^{k(1)}\boldsymbol{\kappa}dA+\frac{1}{2}\int_{\mathcal{A}}\sum_{k=1}^{n}[\mathbf{T}^k\mathbf{L}^T\mathbf{Y}^{k(2)}\boldsymbol{\kappa}]^T\mathbf{L}^T\mathbf{B}^{k(2)}\boldsymbol{\kappa}dA\\&+\int_{\mathcal{A}}(\nabla w+\boldsymbol{\varphi})^T\sum_{k=1}^{n}(\mathbf{L}^T\mathbf{X}^{k(0)}\mathbf{e}+\mathbf{L}^T\mathbf{Y}^{k(0)}\boldsymbol{\kappa})dA\end{aligned} \tag{42}$$

where

$$\mathbf{X}^{k(0)}=-\left[(z_{k+1}-z_k)\mathbf{A}^{k(0)}+\frac{1}{2}(z_{k+1}^2-z_k^2)\mathbf{A}^{k(1)}\right] \tag{43}$$

$$\mathbf{X}^{k(1)}=-\left[\frac{1}{2}(z_{k+1}^2-z_k^2)\mathbf{A}^{k(0)}+\frac{1}{3}(z_{k+1}^3-z_k^3)\mathbf{A}^{k(1)}\right]$$

$$\begin{aligned}\mathbf{Y}^{k(0)}=&-\left[(z_{k+1}-z_k)\mathbf{B}^{k(0)}+\frac{1}{2}(z_{k+1}^2-z_k^2)\mathbf{B}^{k(1)}\right.\\&\left.+\frac{1}{3}(z_{k+1}^3-z_k^3)\mathbf{B}^{k(2)}\right]\end{aligned} \tag{44}$$

$$\begin{aligned}\mathbf{Y}^{k(1)}=&-\left[\frac{1}{2}(z_{k+1}^2-z_k^2)\mathbf{B}^{k(0)}+\frac{1}{3}(z_{k+1}^3-z_k^3)\mathbf{B}^{k(1)}\right.\\&\left.+\frac{1}{4}(z_{k+1}^4-z_k^4)\mathbf{B}^{k(2)}\right]\end{aligned}$$

$$\begin{aligned}\mathbf{Y}^{k(2)}=&-\left[\frac{1}{3}(z_{k+1}^3-z_k^3)\mathbf{B}^{k(0)}+\frac{1}{4}(z_{k+1}^4-z_k^4)\mathbf{B}^{k(1)}\right.\\&\left.+\frac{1}{5}(z_{k+1}^5-z_k^5)\mathbf{B}^{k(2)}\right].\end{aligned}$$

The mixed functional (22) for the model RM2 takes the form

$$\overline{\tilde{H}}(\mathbf{u},w,\boldsymbol{\varphi},\mathbf{e},\boldsymbol{\kappa},\mathbf{N},\mathbf{M})=\tilde{H}^{mb}(\mathbf{u},\boldsymbol{\varphi},\mathbf{e},\boldsymbol{\kappa},\mathbf{N},\mathbf{M})+\overline{\tilde{H}}^s(w,\boldsymbol{\varphi},\mathbf{e},\boldsymbol{\kappa})-\Pi_{\text{ext}}. \tag{45}$$

The number of the unknowns in the FSDT refined RM2 model does not depend on the number of layers; this fact represents an advantageous feature of the proposed RM2 formulation with respect to the RM1 model.

5.3 Refined Model RM3. A possible disadvantage of the refined model RM2 is represented by the large number of unknown functions with respect to the classical full displacement formulation. In fact, functional (45) depends on five displacement parameters $(u_1,u_2,w,\varphi_1,\varphi_2)$, on six midplane strains and curvatures $(e_{11},e_{22},e_{12},\kappa_{11},\kappa_{22},\kappa_{12})$ on six axial and bending resultants $(N_{11},N_{22},N_{12},M_{11},M_{22},M_{12})$.

As matter of fact, in the membrane-bending Hu-Washizu functional $\tilde{H}^{mb}$, defined by Eq. (16), the resultant stress vectors $\mathbf{N}$ and $\mathbf{M}$ can be regarded as the Lagrange multipliers of the constraints corresponding to the compatibility Eqs. (6). The FSDT refined model RM3 is obtained implicitly satisfying the compatibility Eqs. (6) in the membrane-bending Hu-Washizu functional (16); thus, the full displacement membrane-bending functional (23) is obtained. Moreover, the penalty approach is adopted to enforce the constraint (6) in the mixed functional (42); in fact, a penalty term is added into the governing functional, which results in

$$\tilde{\mathcal{E}}(\mathbf{u},w,\boldsymbol{\varphi},\mathbf{e},\boldsymbol{\kappa})=\mathcal{E}^{mb}(\mathbf{u},\boldsymbol{\varphi})+\overline{\tilde{H}}^s(w,\boldsymbol{\varphi},\mathbf{e},\boldsymbol{\kappa})+\Lambda(\mathbf{u},\boldsymbol{\varphi},\mathbf{e},\boldsymbol{\kappa})-\Pi_{\text{ext}} \tag{46}$$

where the penalty term Λ is defined by

$$\Lambda=\frac{1}{2\eta}\int_{\mathcal{A}}[(\mathbf{L}\mathbf{u}-\mathbf{e})^T(\mathbf{L}\mathbf{u}-\mathbf{e})+(\mathbf{L}\boldsymbol{\varphi}-\boldsymbol{\kappa})^T(\mathbf{L}\boldsymbol{\varphi}-\boldsymbol{\kappa})]dA \tag{47}$$

with η the penalty parameter.

According the penalty method, the resultant stresses are deduced as

$$\mathbf{N}=\frac{1}{\eta}(\mathbf{Lu}-\mathbf{e}) \quad \mathbf{M}=\frac{1}{\eta}(\mathbf{L}\boldsymbol{\varphi}-\boldsymbol{\kappa}) \tag{48}$$

5.4 Refined Model RM4. The refined model RM4 is based on the full displacement-based variational formulation. In fact, it is obtained enforcing the strain displacement Eqs. (6) in the shear functional (42). Thus, the functional $\bar{H}^s$-becomes

$$\begin{aligned}\tilde{H}^s=&\int_{\mathcal{A}}\sum_{k=1}^{n}\left\{\frac{1}{2}[\mathbf{T}^k\mathbf{L}^T\mathbf{X}^{k(0)}\mathbf{Lu}]^T+[\mathbf{T}^k\mathbf{L}^T\mathbf{Y}^{k(0)}\mathbf{L}\boldsymbol{\varphi}]^T\right\}\mathbf{L}^T\mathbf{A}^{k(0)}\mathbf{Lu}dA+\int_{\mathcal{A}}\sum_{k=1}^{n}\left\{\frac{1}{2}[\mathbf{T}^k\mathbf{L}^T\mathbf{X}^{k(1)}\mathbf{Lu}]^T+[\mathbf{T}^k\mathbf{L}^T\mathbf{Y}^{k(1)}\mathbf{L}\boldsymbol{\varphi}]^T\right\}\mathbf{L}^T\mathbf{A}^{k(1)}\mathbf{Lu}dA\\&+\frac{1}{2}\int_{\mathcal{A}}\sum_{k=1}^{n}[\mathbf{T}^k\mathbf{L}^T\mathbf{Y}^{k(0)}\mathbf{L}\boldsymbol{\varphi}]^T\mathbf{L}^T\mathbf{B}^{k(0)}\mathbf{L}\boldsymbol{\varphi}dA+\frac{1}{2}\int_{\mathcal{A}}\sum_{k=1}^{n}[\mathbf{T}^k\mathbf{L}^T\mathbf{Y}^{k(1)}\mathbf{L}\boldsymbol{\varphi}]^T\mathbf{L}^T\mathbf{B}^{k(1)}\mathbf{L}\boldsymbol{\varphi}dA\\&+\frac{1}{2}\int_{\mathcal{A}}\sum_{k=1}^{n}[\mathbf{T}^k\mathbf{L}^T\mathbf{Y}^{k(2)}\mathbf{L}\boldsymbol{\varphi}]^T\mathbf{L}^T\mathbf{B}^{k(2)}\mathbf{L}\boldsymbol{\varphi}dA+\int_{\mathcal{A}}(\nabla w+\boldsymbol{\varphi})^T\sum_{k=1}^{n}(\mathbf{L}^T\mathbf{X}^{k(0)}\mathbf{Lu}+\mathbf{L}^T\mathbf{Y}^{k(0)}\mathbf{L}\boldsymbol{\varphi})dA.\end{aligned} \tag{49}$$

Hence, the full displacement functional governing the laminate problem is

$$\tilde{\bar{\mathcal{E}}}(\mathbf{u},w,\boldsymbol{\varphi})=\mathcal{E}^{mb}(\mathbf{u},\boldsymbol{\varphi})+\tilde{H}^s(w,\mathbf{u},\boldsymbol{\varphi})-\Pi_{\text{ext}}. \tag{50}$$

The recovered potential energy functional (50) appears very appealing since it presents only five unknown functions, i.e., u_1, u_2, w, φ_1, and φ_2. On the other hand, second-order derivatives of the in-plane displacement and the rotation vectors, i.e., $\mathbf{u}$ and $\boldsymbol{\varphi}$, appear in the functional $\tilde{\bar{\mathcal{E}}}$. From a numerical point of view, the presence of the second-order derivatives of the unknown functions in the governing functional could represent a drawback. In fact, in the perspective of developing suitable finite laminate elements based on refined FSDT theories, a greater continuity of the interpolation functions is required.

6 Numerical Applications

With the aim of verifying the accuracy of the proposed FSDT refined models, some numerical calculations are developed. Results are carried out for homogeneous plates as well as for composite laminates. In particular, square plates, characterized by the in-plane dimension a and subjected to transversal sinusoidal loading, are considered. The laminates have the side to thickness ratio $\rho=h/a=0.10$. The following elastic properties are introduced in the computations:

$$\frac{E_L}{E_T}=25, \quad \nu_{LT}=0.25, \quad \frac{G_{LT}}{E_T}=0.5, \quad \frac{G_{TT}}{E_T}=0.2 \tag{51}$$

which correspond to a strongly orthotropic graphite-epoxy material. The subscripts $_L$ and $_T$ indicate the longitudinal and transversal principal material directions.

6.1 Cylindrical Bending. Initially, homogeneous and cross-ply laminated plates in cylindrical bending, subjected to the sinusoidal load $p=p_0\sin(\alpha x)$ with $\alpha=\pi/a$, are studied. In particular, antisymmetric [0/90] and symmetric [0/90/0] laminates are considered. In Table 1, the results obtained using the refined models are put in comparison with the exact three-dimensional analytical solution (3D_AS) obtained by Pagano [33] and with those recovered through the classical Mindlin-Reissner theory (FSDT). In particular, FSDT solutions are obtained considering the shear corrector factor χ equal to $\chi_0=5/6$ and the exact value of shear corrector factor proposed by Whitney χ_W, [8]. Results are reported in terms of the dimensionless maximum displacement $w_{\max}$ defined as

$$w_{\max}=100\frac{E_T w_C}{p_0 h\rho^4} \tag{52}$$

where w_C represents the transversal displacement occuring in the center of the laminate, i.e. $w_C=w(a/2,a/2)$.

It is apparent the effectiveness of the refined models RM2, RM3, and RM4. In fact, RM2, RM3, and RM4 results are in perfect agreement with the FSDTχ_W and 3D_AS solutions; in other words, the RM2, RM3, and RM4 approaches are able to recover the FSDTχ_W model without the use of the shear correction factors. Moreover, the RM1 appears satisfactory for the homogeneous plate and for the antisymmetric [0/90] laminate, while it is absolutely unsatisfactory when the symmetric [0/90/0] laminate is considered.

In Fig. 1 the dimensionless shear stress profile τ_{1z}/p_0 for the homogeneous plate in cylindrical bending is reported. The results obtained by the four proposed refined models, i.e., RM1, RM2, RM3, and RM4, are compared with the shear stress derived by the analytical three-dimensional solution. It can be noted the perfect agreement between all the computed solutions with the exact three-dimensional solution.

Then, the homogeneous plate in cylindrical bending is studied considering fictitious staking sequences of one layer [0], three equal layers [0/0/0] and ten equal layers [0/0/0/0/0/0/0/0/0/0]. Results in terms of dimensionless shear stress profile τ_{1z}/p_0 in the plate thickness are reported in Fig. 2. It can be noted that the RM2, RM3 and RM4 proposed models lead all to the same solution in perfect agreement with the exact three-dimensional solution. On the contrary, the RM1 model gives different solutions depending on the number of layers considered for the fictitious staking sequence. In particular, for $n=10$ the shear stress is almost constant in the core of the plate. In fact, increasing the number of layers, i.e., increasing the number of independent functions approximating the shear stresses, the constitutive Eq. (9) tends to be enforced. Thus, enlarging the space of the shear parameters $\mathbf{t}_o^2,..,\mathbf{t}_o^n,\mathbf{t}^1,..,\mathbf{t}^n$ the shear stress profile tends to become constant for the homogeneous plate.

Table 1 Dimensionless maximum displacement $w_{\max}$ defined by formula (52) for homogeneous plate and for [0/90] and [0/90/0] composite laminates in cylindrical bending

$w_{\max}$	Homogeneous	[0/90]	[0/90/0]
FSDTχ_0	0.7347060	2.9662221	0.8136198
FSDTχ_W	0.7347060	2.9713422	0.9443031
RM1	0.7347060	2.9482925	0.7902380
RM2	0.7347060	2.9722354	0.9443031
RM3	0.7347060	2.9722354	0.9443031
RM4	0.7347033	2.9721543	0.9443031
3D_AS	0.7316710	2.9502480	0.9306170

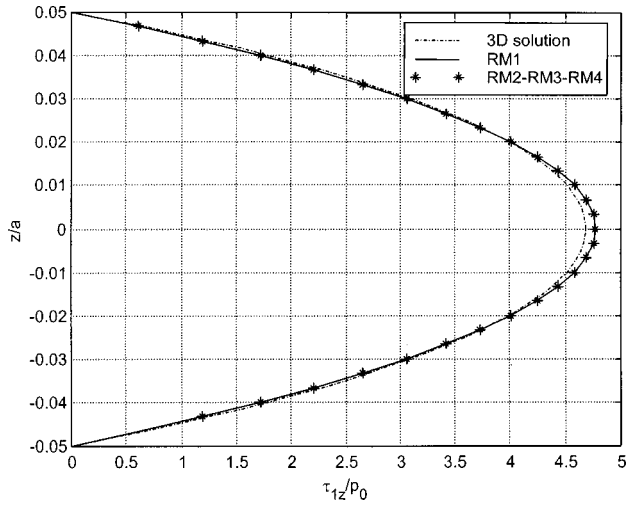

Fig. 1 Dimensionless shear stress τ_{1z}/p_0 at $x_1=0$ for homogeneous plate in cylindrical bending; comparison between the different solutions

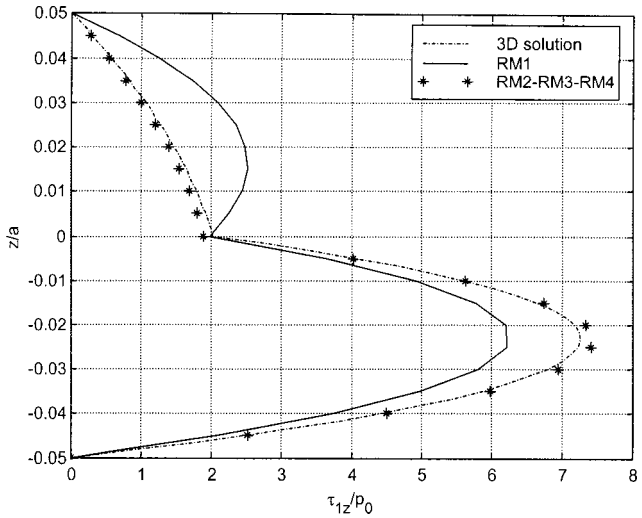

Fig. 3 Dimensionless shear stress τ_{1z}/p_0 at $x_1=0$ for the [0/90] laminate in cylindrical bending; comparison between the different solutions

In Figs. 3 and 4 the dimensionless shear stresses τ_{1z}/p_0 are plotted for the [0/90] and [0/90/0] laminates, respectively. Again it can be noted the good agreement between the solutions obtained using the RM2, RM3, and RM4 models and the three-dimensional analytical solution. On the contrary, the RM1 model, based on the assumption of independent approximation of the shear stresses, leads to unsatisfactory solution, since the profile appears absolutely inadequate.

6.2 Simply Supported Laminates

Cross-Ply Laminates. Cross-ply laminates subjected to the sinusoidal load $p=p_0\sin(\alpha x)\sin(\alpha y)$ with $\alpha=\pi/a$, are considered. The following SS1 boundary conditions are adopted:

$$u_2=w=\varphi_2=0 \quad N_{11}=M_{11}=0 \quad \text{at } x_1=0 \quad \text{and} \quad x_1=a$$

$$u_1=w=\varphi_1=0 \quad N_{22}=M_{22}=0 \quad \text{at } x_2=0 \quad \text{and} \quad x_2=a.$$

Results are computed for homogeneous plate and for [0/90] and [0/90/0] laminates.

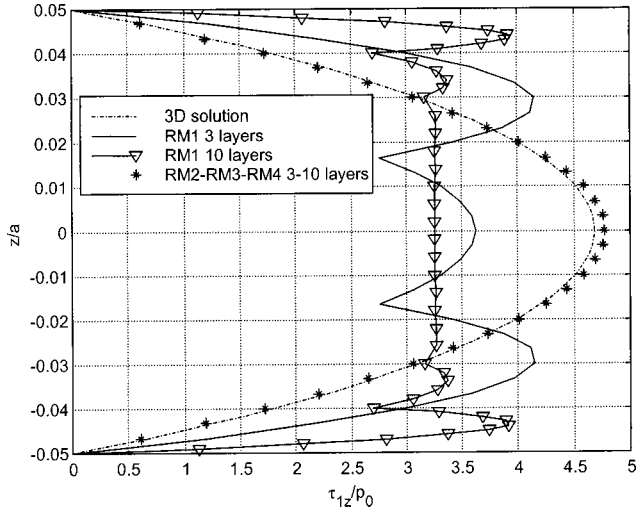

Fig. 2 Dimensionless shear stress τ_{1z}/p_0 at $x_1=0$ for homogeneous plate in cylindrical bending; comparison between the different solutions computed considering one, three, and ten equal layers

In Table 2 the dimensionless maximum displacement $w_{\max}$ defined by formula (52) is reported; in particular, results are obtained, considering

- the classical FSDT analytical solution with $\chi=\chi_0=5/6$,
- the finite element solution (FEMχ_0) with $\chi=\chi_0$,

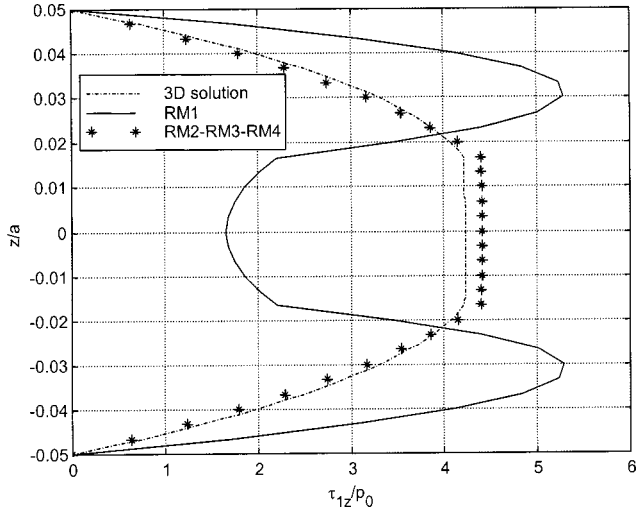

Fig. 4 Dimensionless shear stress τ_{1z}/p_0 at $x_1=0$ for the [0/90] laminate in cylindrical bending; comparison between the different solutions

Table 2 Dimensionless maximum displacement $w_{\max}$ defined by formula (52) for homogeneous plate and for [0/90] and [0/90/0] cross-ply laminates

$w_{\max}$	Homogeneous	[0/90]	[0/90/0]
FSDTχ_0	0.6382997	1.237270	0.669302
FEMχ_0	0.63834	1.2373	0.66930
FEMχ	0.63834	1.2319	0.76377
RM1	0.6382997	-	-
RM2	0.6382997	1.231817	0.763779
RM3	0.6382997	1.231817	0.763779
RM4	0.6382997	1.231817	0.763779
3D	0.6338085	1.224799	0.751425

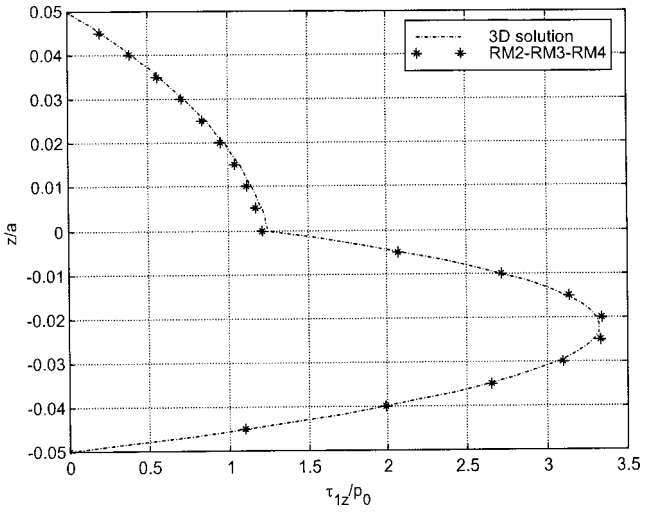

Fig. 5 Dimensionless shear stress τ_{1z}/p_0 for the [0/90] laminate computed at $x_1=0$, $x_2=a/2$; comparison with the three-dimensional analytical solution

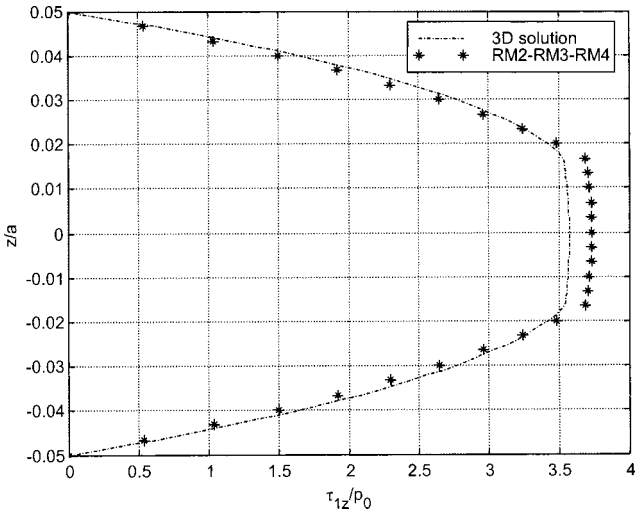

Fig. 7 Dimensionless shear stress τ_{1z}/p_0 for the [0/90/0] laminate computed at $x_1=0$, $x_2=a/2$; comparison with the three-dimensional analytical solution

- the finite element solution (FEMχ) with exact value of the shear correction factor computed by the iterative procedure proposed in [13],
- the RM1 analytical solution only for the homogeneous plate,
- the RM2, RM3, and RM4 analytical solutions, and
- the exact three-dimensional solution 3D-AS.

In Figs. 5 and 6 the dimensionless shear stress profiles τ_{1z}/p_0 and τ_{2z}/p_0 for the [0/90] laminate are plotted, respectively. Analogously, in Figs. 7 and 8 the shear stress profiles are plotted for the [0/90/0] laminate. It can be noted that the proposed models are able to approximate very accurately the exact three-dimensional solution for both the considered laminations.

Finally, in Fig. 9 the dimensionless displacement $w_{\max}$ defined by formula (52), computed for the [0/90/0] lamination, is plotted versus the ratio $\rho=h/a$. In particular, the RM3 solution is compared with three dimensions with the FSDTχ_0, with the FSDTχ and with the classical laminate theory (CLT) solutions. It can be emphasized the good accordance between the RM3 and the analytical three-dimensional solutions for a wide range of the ratio ρ.

Angle-Ply Laminate. The antisymmetric [−45/45] angle-ply laminate subjected to the sinusoidal load $p=p_0\sin(\alpha x)\sin(\alpha y)$ with $\alpha=\pi/a$, is considered. The following SS2 boundary conditions are adopted:

$$u_1=w=\varphi_2=0 \quad N_{12}=M_{11}=0 \quad \text{at } x_1=0 \quad \text{and} \quad x_1=a$$

$$u_2=w=\varphi_1=0 \quad N_{12}=M_{22}=0 \quad \text{at } x_2=0 \quad \text{and} \quad x_2=a.$$

In Table 3 the dimensionless maximum displacement $w_{\max}$ defined by formula (52) is reported; in particular, results are obtained, considering

- the classical FSDT analytical solution with $\chi=\chi_0$ and
- the RM2, RM3, and RM4 analytical solutions.

It can be noted that the RM2, RM3, and RM4 models give all the same results which differ from the FSDT solution obtained adopting the shear correction factor $\chi=5/6$. Finally, in Fig. 10 the shear stress profile τ_{1z}/p_0 for the angle-ply laminate is plotted.

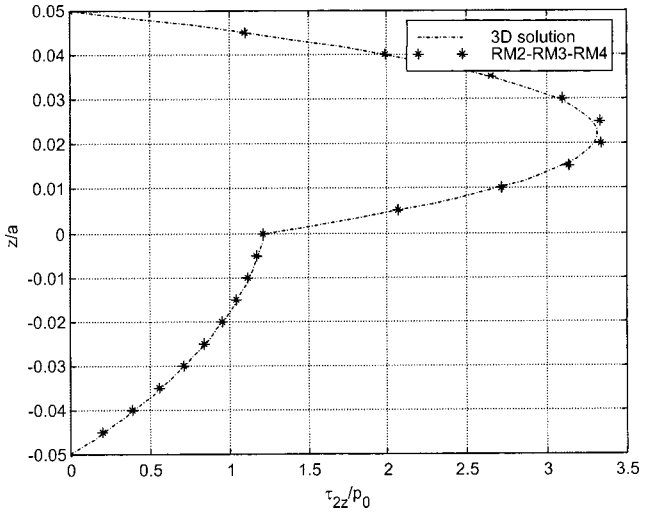

Fig. 6 Dimensionless shear stress τ_{2z}/p_0 for the [0/90] laminate computed at $x_1=a/2$, $x_2=0$; comparison with the three-dimensional analytical solution

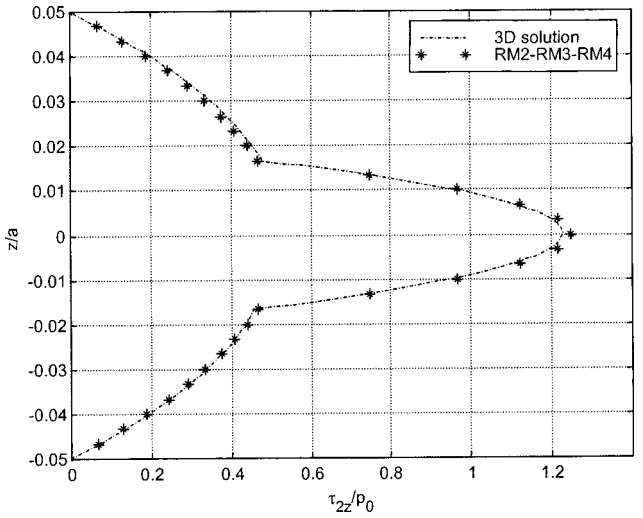

Fig. 8 Dimensionless shear stress τ_{2z}/p_0 for the [0/90/0] laminate computed at $x_1=a/2$, $x_2=0$; comparison with the three-dimensional analytical solution

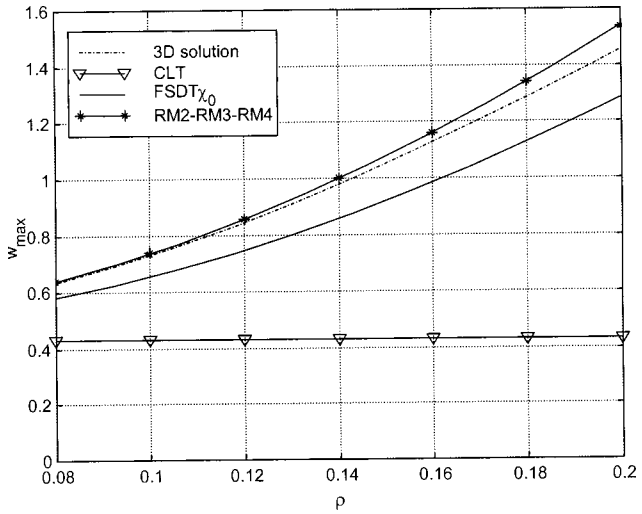

Fig. 9 Dimensionless displacement w_{max} versus the thickness to side ratio

7 Conclusions

Refined laminate models are presented. They are derived considering mixed variational formulations of the laminate problem, introducing suitable representation forms of the shear stresses in the plate thickness. It is obtained that independent approximations of the shear stresses can lead to unsatisfactory models, which are not able to recover the correct profiles of the stresses.

The proposed RM2, RM3, and RM4 models, obtained representing the transverse shear stress profile by using the three-dimensional equations, are very satisfactory; in fact, the solutions obtained by these models are in very good accordance with the three-dimensional analytical solution.

The RM2 approach appears the more suitable in view to develop effective laminate finite elements. In fact, the RM3 model needs the use of a penalty parameter, which is not always simple to set; on the other hand, the RM4 requires the use of smoother approximation functions in the finite element formulation, since second-order derivatives appear in the governing functional.

The proposed model does not suffer of any limitation about the number of layers defining the stacking sequence and of the ply angles; more complex situations can be investigated, including quasi-isotropic laminates. More complex cases can be studied developing suitable finite elements based on the proposed formulations. In fact, the presented mixed principles, in particular the RM2 model, are the bases for the development of new and performing finite elements. One of the major problems in developing mixed laminate finite elements, is the definition of the approximation functions used for the midplane strains and curvatures in order to verify the stability requirement, related to the LBB condition. Finally, full displacement finite elements can be recovered from the refined model RM2 performing static condensation of strain and stress variables.

Table 3 Dimensionless maximum displacement w_{max} defined by formula (52) for the [−45/45] angle-ply composite laminate

Model	FSDTχ_0	RM2	RM3	RM4
w_{max}	0.8828107	0.8929168	0.8929168	0.8929168

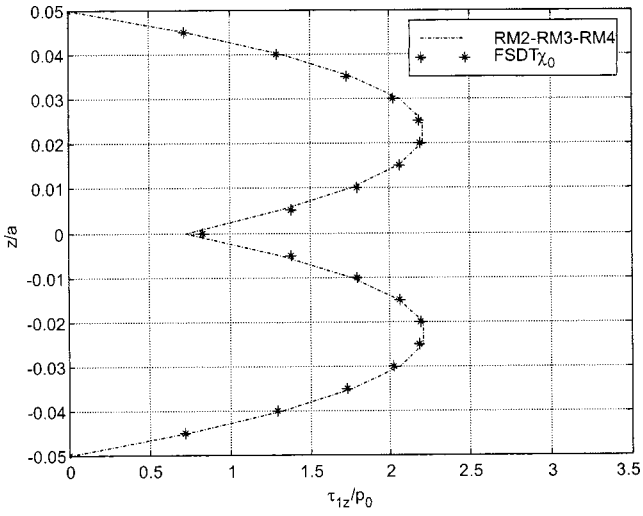

Fig. 10 Dimensionless shear stress τ_{1z}/p_0 for the [−45/45] laminate computed at $x_1=0$, $x_2=a/2$; comparison with first-order shear deformation theory ($\chi=5/6$) analytical solution

References

[1] Ochoa, O. O., and Reddy, J. N., 1992, *Finite Element Analysis of Composite Laminates*, Kluwer, Dordrecht, The Netherlands.

[2] Reddy, J. N., 1997, *Mechanics of Laminated Composite Plates, Theory and Analysis*, CRC Press, Boca Raton, FL.

[3] Reissner, E., and Stavsky, Y., 1961, "Bending and Stretching of Certain Types of Heterogeneous Aeolotropic Elastic Plates," ASME J. Appl. Mech., **28**, pp. 402–412.

[4] Ambartsumyan, S. A., 1970, *Theory of Anisotropic Plates*, Technomic, Lancaster, PA.

[5] Reissner, E., 1945, "The Effect of Transverse Shear Deformation on the Bending of Elastic Plates," ASME J. Appl. Mech., **12**, pp. 69–77.

[6] Mindlin, R. D., 1951, "Influence of Rotatory Inertia and Shear on Flexural Motions of Isotropic, Elastic Plates," ASME J. Appl. Mech., **38**, pp. 31–38.

[7] Yang, P. C., Norris, C. H., and Stavsky, Y., 1996, "Elastic Wave Propagation in Heterogeneous Plates," Int. J. Solids Struct., **2**, pp. 665–684.

[8] Whitney, J. M., and Pagano, N. J., 1970, "Shear Deformation in Heterogeneous Anisotropic Plates," ASME J. Appl. Mech., **37**, pp. 1031–1036.

[9] Whitney, J. M., 1973, "Shear Correction Factors for Orthotropic Laminates Under Static Load," ASME J. Appl. Mech., **40**, pp. 302–304.

[10] Noor, A. K., and Burton, W. S., 1990, "Assessment of Computational Models for Multilayered Anisotropic Plates," Comput. Struct., **14**, pp. 233–265.

[11] Noor, A. K., Burton, W. S., and Peters, J. M., 1990, "Predictor-Corrector Procedures for Stress and Free Vibration Analyses of Multilayered Composite Plates and Shells," Comput. Methods Appl. Mech. Eng., **82**, pp. 341–363.

[12] Noor, A. K., Burton, W. S., and Bert, C. W., 1996, "Computational Model for Sandwich Panels and Shells," Appl. Mech. Rev., **49**, pp. 155–199.

[13] Auricchio, F., and Sacco, E., 1999, "A Mixed-Enhanced Finite Element for the Analysis of Laminated Composite Plates," Int. J. Numer. Methods Eng., **44**, pp. 1481–1504.

[14] Alfano, G., Auricchio, F., Rosati, L., and Sacco, E., 2001, "MITC Finite Elements for Laminated Composite Plates," Int. J. Numer. Methods Eng., **50**, pp. 707–738.

[15] Pai, P. F., 1995, "A New Look at the Shear Correction Factors and Warping Functions of Anisotropic Laminates," Int. J. Solids Struct., **32**, pp. 2295–2313.

[16] Yunquin, Q., and Knight, N. F. Jr., 1996, "A Refined First-Order Shear-Deformation Theory and Its Justification by Plane-Strain Bending Problem of Laminated Plates," Int. J. Solids Struct., **33**, pp. 49–64.

[17] Rolfes, R., and Rohwer, K., 1997, "Improved Transverse Shear Stresses in Composite Finite Element Based on First Order Shear Deformation Theory," Int. J. Numer. Methods Eng., **40**, pp. 51–60.

[18] Rolfes, R., 1998, "Evaluation of Transverse Thermal Stresses in Composite Plates Based on First Order Shear Deformation Theory," Comput. Methods Appl. Mech. Eng., **167**, pp. 355–368.

[19] Lo, K. H., Christensen, R. M., and Wu, E. M., 1978, "A High-Order Theory of Plate Deformation. Part II: Laminated Plates," ASME J. Appl. Mech., **44**, pp. 669–676.

[20] Reddy, J. N., 1984, "A Simple High-Order Theory for Laminated Composite Plates," ASME J. Appl. Mech., **51**, pp. 745–752.

[21] Seide, P., 1980, "An Improved Approximate Theory for Bending of Laminated Plates," Mech. Today, **5**, pp. 451–466.

[22] Reddy, J. N., 1987, "A Generalization of Two-Dimensional Theories of Laminated Plates," Commun. Appl. Numer. Methods **3**, pp. 173–180.

[23] Reddy, J. N., 1990, "On Refined Theories of Composite Laminates," Meccanica, **25**, pp. 230–238.

[24] Reddy, J. N., Barbero, E. J., and Teply, J. L., 1990, "An Accurate Determination of Stresses in Thick Laminates Using a Generalized Plate Theory," Int. J. Numer. Methods Eng., **29**, pp. 1–14.

[25] Bisegna, P., and Sacco, E., 1997, "A Layer-Wise Laminate Theory Rationally Deduced From Three-Dimensional Elasticity," ASME J. Appl. Mech., **64**, pp. 538–544.

[26] Barbero, E. J., 1992, "3-D Finite Element for Laminated Composites With 2-D

Kinematic Constraints,'' Comput. Struct., **45**, pp. 263–271.
[27] Di Sciuva, M., and Icardi, U., 1993, ''Discrete-Layer Models for Multilayered Shells Accounting for Interlayer Continuity,'' Meccanica, **28**, pp. 281–291.
[28] Carrera, E., 1999, ''Multilayered Shell Theories Accounting for a Layer-Wise Mixed Description. Part I. Governing Equations. Part II. Numerical Evaluations,'' AIAA J., **37**, pp. 1117–1124.
[29] Aitharaju, V. R., and Averill, R. C., 2000, ''C^0 Zig-Zag Kinematic Displacement Models for the Analysis of Laminated Composites,'' Mech. Compos. Mat. Struct., **6**, pp. 31–56.
[30] Carrera, E., 2001, ''Developments, Ideas, and Evaluations Based Upon Reissner's Mixed Variational Theorem in the Modeling of Multilayered Plates and Shells,'' Appl. Mech. Rev., **54**, pp. 301–328.
[31] Maenghyo, Cho, and Min-Ho, Kim, 1996, ''A Postprocess Method Using a Displacement Field of Higher-Order Shell Theory,'' Compos. Struct., **34**, pp. 185–196.
[32] Rolfes, R., Rohwer, K., and Ballerstaedt, M., 1998, ''Efficient Linear Transverse Normal Stress Analysis of Layered Composite Plates,'' Compos. Struct. , **68**, pp. 643–652.
[33] Pagano, N. J., 1970, ''Exact Solutions for Rectangular Bidirectional Composites and Sandwich Plates,'' J. Compos. Mater., **4**, pp. 20–34.
[34] Bisegna, P., and Sacco, E., 1997, ''A Rational Deduction of Plate Theories From the Three-Dimensional Linear Elasticity,'' Z. Angew. Math. Mech., **77**, pp. 349–366.
[35] Auricchio, F., and Sacco, E., 1999, ''Partial-Mixed Formulation and Refined Models for the Analysis of Composite Laminates Within a FSDT,'' Compos. Struct., **46**, pp. 103–113.